LRIT3 Differentially Affects Connectivity and Synaptic Transmission of Cones to ON- and OFF-Bipolar Cells

Marion Neuillé,[1] Yan Cao,[2] Romain Caplette,[1] Debbie Guerrero-Given,[3] Connon Thomas,[3] Naomi Kamasawa,[3] José-Alain Sahel,[1,4–8] Christian P. Hamel,[9] Isabelle Audo,[1,4,5] Serge Picaud,[1] Kirill A. Martemyanov,[2] and Christina Zeitz[1]

[1]Sorbonne Universités, UPMC Univ Paris 06, INSERM U968, CNRS UMR 7210, Institut de la Vision, Paris, France
[2]Department of Neuroscience, The Scripps Research Institute, Jupiter, Florida United States
[3]Max Planck Florida Institute for Neuroscience, Jupiter, Florida United States
[4]CHNO des Quinze-Vingts, DHU Sight Restore, INSERM-DHOS CIC1423, Paris, France
[5]Institute of Ophthalmology, University College of London, London, United Kingdom
[6]Fondation Ophtalmologique Adolphe de Rothschild, Paris, France
[7]Académie des Sciences–Institut de France, Paris, France
[8]Department of Ophthalmology, The University of Pittsburgh School of Medicine, Pittsburgh, United States
[9]INSERM U583, Physiopathologie et thérapie des déficits sensoriels et moteurs, Institut des Neurosciences de Montpellier, Hôpital Saint-Eloi, Montpellier, France

Correspondence: Christina Zeitz, Institut de la Vision, Department of Genetics, 17 Rue Moreau, Paris 75012, France; christina.zeitz@inserm.fr.

Submitted: September 13, 2016
Accepted: February 28, 2017

Citation: Neuillé M, Cao Y, Caplette R, et al. LRIT3 differentially affects connectivity and synaptic transmission of cones to ON- and OFF-bipolar cells. *Invest Ophthalmol Vis Sci*. 2017;58:1768–1778. DOI:10.1167/iovs.16-20745

Purpose. Mutations in *LRIT3* lead to complete congenital stationary night blindness (cCSNB). Using a cCSNB mouse model lacking *Lrit3* (*nob6*), we recently have shown that LRIT3 has a role in the correct localization of TRPM1 (transient receptor potential melastatin 1) to the dendritic tips of ON-bipolar cells (BCs), contacting both rod and cone photoreceptors. Furthermore, postsynaptic clustering of other mGluR6 cascade components is selectively eliminated at the dendritic tips of cone ON-BCs. The purpose of this study was to further define the role of LRIT3 in structural and functional organization of cone synapses.

Methods. Exhaustive electroretinogram analysis was performed in a patient with *LRIT3* mutations. Multielectrode array recordings were performed at the level of retinal ganglion cells in *nob6* mice. Targeting of GluR1 and GluR5 at the dendritic tips of OFF-BCs in *nob6* retinas was assessed by immunostaining and confocal microscopy. The ultrastructure of photoreceptor synapses was evaluated by electron microscopy in *nob6* mice.

Results. The patient with *LRIT3* mutations had a selective ON-BC dysfunction with relatively preserved OFF-BC responses. In *nob6* mice, complete lack of ON-pathway function with robust, yet altered signaling processing in OFF-pathways was detected. Consistent with these observations, molecules essential for the OFF-BC signaling were normally targeted to the synapse. Finally, synaptic contacts made by ON-BC but not OFF-BC neurons with the cone pedicles were disorganized without ultrastructural alterations in cone terminals, horizontal cell processes, or synaptic ribbons.

Conclusions. These results suggest that LRIT3 is likely involved in coordination of the transsynaptic communication between cones and ON-BCs during synapse formation and function.

Keywords: retina, congenital stationary night blindness, LRIT3, electron microscopy, multielectrode array

The first steps in vision occur when rod and cone photoreceptors transform light into an electrical signal, which is then transmitted to other retinal neurons for processing. Photoreceptors respond to light with a graded hyperpolarization that suppresses the glutamate release at their terminals. Both rods and cones make synaptic contacts with bipolar cells (BCs). There are two types of BCs: ON- and OFF-BCs, expressing different sets of glutamate receptors and responding differently to light. ON-BCs express the metabotropic glutamate receptor 6 (GRM6/mGluR6)[1–3] and depolarize in response to light via a signaling cascade that opens the transient receptor potential melastatin 1 (TRPM1) cation channel.[4–6] OFF-BCs express ionotropic glutamate receptors[7–10] and hyperpolarize in response to light. In the outer plexiform layer (OPL), ON-BCs make synaptic contacts with both rod spherules and cone pedicles. ON-BC dendrites invaginate photoreceptor terminals and form triads with invaginating horizontal cell processes. OFF-BCs make flat contacts only at cone pedicles.[11,12]

ON/OFF dichotomy set at the level of the signal segregation through ON- and OFF-BCs is preserved in the retinal ganglion cells (RGCs), the output neurons of the retina, and extends to the visual cortex. ON-RGCs have a spiking activity at light onset, whereas OFF-RGCs spike at light offset. A third type of

RGCs, named ON/OFF-RGCs, exhibits both types of responses.[13] ON- and OFF-RGCs receive afferents from cones through cone ON- and OFF-BCs, respectively. The rod input to RGCs is indirect and proceeds through rod BCs contacting AII amacrine cells,[14] which in turn form synapses onto the axon terminals of cone BCs. This ON/OFF dichotomy allows the retina to optimally respond to contrasts rather than only to absolute luminance.[15]

The complete form of congenital stationary night blindness (cCSNB) is a group of retinal disorders associated with defect in the signal transmission via ON-pathways. To date, several mouse models for cCSNB have been described with mutations in genes coding for proteins localized at the dendritic tips of ON-BCs and implicated in the mGluR6 signaling cascade.[3–6,16–23] We have recently discovered a new gene mutated in cCSNB, *LRIT3*,[24] and developed a corresponding knockout mouse model, *nob6*.[25] Similar to other mouse models for cCSNB, *nob6* mice display a "no b-wave" (*nob*) phenotype when evaluated by full-field electroretinogram (ERG) and have normal retinal structure.[25] This phenotype differs from the phenotype observed in mouse models for incomplete CSNB resulting from both ON- and OFF-pathway dysfunction, showing reduced or absent cone ERGs and some structural defects including thinner OPL and development of ectopic dendrites from ON-BCs and horizontal cells.[26] Although the exact role of LRIT3 in the mGluR6 signaling cascade remains to be elucidated, we have previously shown that LRIT3 is important for the correct localization of TRPM1 at the dendritic tips of ON-BCs.[27] More surprisingly, *nob6* retinas show a unique feature with almost complete elimination of postsynaptic clustering of mGluR6 cascade components at the dendritic tips of cone ON-BCs despite their undisrupted accumulation at the dendritic tips of rod BCs.[27] These deficits suggest a potential involvement of LRIT3 in cone synapse formation and signaling to ON- and OFF-BCs.

Here we investigated the role of LRIT3 in structural and functional organization of cone synapses in a patient and *nob6* mice mutated in *LRIT3*.

Materials and Methods

Ethics Statements

For humans, research procedures were conducted in accordance with institutional guidelines and the Declaration of Helsinki. Informed consent was obtained from participating members and parents (on behalf of children).

All animal procedures were performed according to the Council Directive 2010/63EU of the European Parliament and the Council of September 22, 2010, on the protection of animals used for scientific purposes, with the National Institutes of Health guidelines and with the ARVO Statement for the Use of Animals in Ophthalmic and Vision Research. They were approved by the French Minister of National Education, Superior Education and Research (authorization 02342.02 delivered on January 26, 2016) and were granted formal approval by the Institutional Animal Care and Use Committee of the Scripps Research Institute.

Full-Field ERG Recordings in Patient

A 13-year-old female patient affected with cCSNB with compound heterozygous disease causing mutations (c.1151C>G, p.(Ser384*); c.1538_1539del, p.(Ser513Cysfs*59) in *LRIT3* (NM_198506)[24] was called back for additional recordings. Full-field ERG incorporating the International Society for Clinical Electrophysiology of Vision (ISCEV) standards was performed.[28] ON-OFF ERG responses were recorded as previously described.[29]

Animal Care

The generation and characterization of the *Lrit3* knockout mouse model (http://www.taconic.com/knockout-mouse/lrit3; in the public domain) has been described elsewhere.[25] Six mutant (*Lrit3*$^{nob6/nob6}$) 6- to 16-week-old mice of both sexes and six age-matched controls were used in this study. From each group, three retinas were used for multielectrode array (MEA) with a total of 231 recorded cells from control retinas and 109 recorded cells from mutant retinas: one retina was used for immunostaining and two retinas were used for electron microscopy. Mice were housed in groups in a temperature-controlled room with a 12-hour light/12-hour dark cycle. Fresh water and rodent diet were available ad libitum.

Multielectrode Array

Multielectrode array recordings were obtained from ex vivo isolated flat-mounted retina as previously described.[30] Mice were killed by CO_2 inhalation followed by cervical dislocation, and eyes were briefly enucleated and dissected under dim red light at room temperature in Ames medium (Sigma-Aldrich Corp., St. Louis, MO, USA), oxygenated with 95% O_2 and 5% CO_2 (Air Liquide, Paris, France). Retinas were placed on a Spectra/Por membrane (Spectrum Laboratories, Rancho Dominguez, CA, USA) and gently pressed against an MEA (MEA256 100/30 iR-ITO; Multi Channel Systems MCS, Reutlingen, Germany) by using a micromanipulator, with RGCs facing the electrodes. Retinas were continuously perfused with bubbled Ames medium at 34°C at a rate of 1 to 2 mL/min and let to rest for 1 hour before the recording session.[30] Under dark conditions, 10 repeated full-field light stimuli at a 480 nm-wavelength were applied to the samples at 10^{14} photons/cm^2/s for 2 seconds with 10-second interval by using a Polychrome V monochromator (Olympus, Hamburg, Germany) driven by an STG2008 stimulus generator (MCS). Raw RGC activity recorded by MEA was amplified (gain 1000–1200) and sampled at 20 kHz by using MCRack software (MCS). Resulting data were stored and filtered with a 200-Hz high-pass filter. Raster plots were obtained by using a combination of threshold detection, template matching, and cluster grouping based on principal component analysis using Spike2 v.7 software (CED Co., Cambridge, UK). Peristimulus time histograms were plotted with a bin size of 50 ms by using a custom-made script in MATLAB v.R2014b (MathWorks, Inc., Natick, MA, USA). Only RGCs with a mean spontaneous firing frequency superior to 1 Hz were considered. We subsequently determined for each sorted RGC the maximum firing frequency in an interval of 2 seconds after light onset (for ON-responses) and in an interval of 2 seconds after light offset (for OFF-responses). These values were normalized to the mean spontaneous firing frequency of the corresponding RGC. Considering that significant responses have a maximum firing frequency that is superior to the mean spontaneous firing frequency + 5 SD, we determined the time at which these significant frequencies were reached after the light onset for ON-responses and after the light offset for OFF-responses. The histograms were traced with GraphPad Prism v.6 (GraphPad Software, La Jolla, CA, USA).

Statistical Analyses

Statistical analyses were performed with GraphPad Prism v.6 for MEA studies. Mann-Whitney *U* test was used to compare the maximum firing rates for ON- and OFF-responses between

wild-type and mutant mice, respectively. Kruskal-Wallis test was used to compare the times at which the significant rates were reached among ON-responses for wild-type mice and OFF-responses for wild-type and mutant mice. Post hoc comparisons were used to compare the conditions two by two when the Kruskal-Wallis test permitted rejection of the hypothesis H0. Tests were considered as significant when $P < 0.05$.

Preparation of Retinal Sections for Immunohistochemistry

Mice were killed by CO_2 administration and cervical dislocation. Eyes were removed and prepared as previously described[27] with some modifications. The anterior segment and lens were removed and the eyecup was fixed in 2% (wt/vol) paraformaldehyde in 0.12 M phosphate buffer, pH 7.2 (PB) for 10 minutes at room temperature. The eyecup was washed three times in PB and cryoprotected with increasing concentrations of ice-cold sucrose in PB (10%, 20% for 1 hour each and 30% overnight). Subsequently, the eyecup was embedded in 7.5% gelatin–10% sucrose and frozen in a dry ice–cooled bath of isopentane. Sections were cut at a thickness of 16 µm on a cryostat and mounted onto glass slides (Super-Frost; Thermo Fisher Scientific, Waltham, MA, USA). The slides were air dried and stored at −80°C.

Immunostaining of Retinal Cryosections

Immunostaining on retinal sections was performed as previously described[27] with some modifications. Sections were incubated with primary antibodies in 3% (vol/vol) normal donkey serum, 1% bovine serum albumin, and 0.5% Triton X-100 in PB overnight at room temperature. Primary antibodies were as follows: rabbit anti-GluR1 (1:100, AB1504; Merck, Darmstadt, Germany), goat anti-GluR5 (1:100, sc-7616; Santa-Cruz Biotechnology, Dallas, TX, USA), rabbit anti-pikachurin (1:1000, 011-22631; Wako, Osaka, Japan), and mouse anti–PSD-95 (1:500, MABN68; Merck). After washing in PB, the sections were incubated with secondary antibodies coupled to Alexa Fluor 488 or Cy3 (Jackson ImmunoResearch, West Grove, PA, USA) at a dilution of 1:1000 in PB for 1.5 hours at room temperature. The slides were stained with 4′,6-diamidino-2-phenylindole (DAPI) and subsequently coverslipped with mounting medium (Mowiol; Merck Millipore, Billerica, MA, USA). None of the secondary antibodies used gave recordable signal when used without primary antibodies (data not shown).

Image Acquisition

Fluorescent staining signals were captured with a confocal microscope (FV1000; Olympus, Hamburg, Germany) equipped with 405-, 488-, and 559-nm lasers. Confocal images were acquired with a 40× objective compatible with oil (lens numerical aperture: 1.3) imaging pixels of 310 nm and 77 nm in width and height for zoom 1 and 4, respectively, and using a 0.52-µm step size. Each image corresponds to the projection of three optical sections. For figures, brightness and contrast were optimized (ImageJ v.1.50; http://imagej.nih.gov/ij/; provided in the public domain by National Institutes of Health, Bethesda, MD, USA).

Electron Microscopy

Eyes were enucleated, cleaned of extraocular tissue, and prefixed for 15 minutes in cacodylate-buffered half-Karnovsky's fixative containing 2 mM calcium chloride. Then the eyecups were hemisected along the vertical meridian and fixed overnight in the same fixative. The specimens were rinsed with cacodylate buffer and postfixed in 2% osmium tetroxide in buffer for 1 hour, then gradually dehydrated in an increasing ethanol and acetone series (30%–100%), and embedded in Durcupan ACM resin (Electron Microscopy Sciences, Hatfield, PA, USA). Blocks were cut to 70-nm thickness and were stained with 0.5% lead citrate. Sections were examined in a Tecnai G2 spirit BioTwin (FEI, Hillsboro, OR, USA) transmission electron microscope at 80 or 100-kV accelerating voltage. Images were captured with a Veleta CCD camera (Olympus, Tokyo, Japan) operated by TIA software (FEI).

Results

OFF-BC Responses Are Preserved With Selective Defect in ON-BC Responses in a Patient With cCSNB Due To *LRIT3* Mutations

Recently, we observed selective elimination of postsynaptic molecules at the dendritic tips of cone ON-BCs in addition to the absence of TRPM1 at both rod and cone ON-BCs. To evaluate if this influences the function of OFF-BCs synapsing with cones, we clinically reinvestigated a patient with *LRIT3* mutations.[24] Similar to previously described evaluation of this patient,[24] we detected no recordable responses to dark-adapted 0.01 ERG recordings, and an electronegative waveform was observed at both dark-adapted 3.0 and 10.0 ERGs. Light-adapted 3.0 ERGs and 3.0 flicker ERGs were also in accordance with a stationary isolated ON-defect and consistent with the previous diagnostic description of cCSNB[24] (Fig. 1).

To separately study ON- and OFF-BC responses, we used long-duration stimulations under photopic conditions (Fig. 1). Recordings revealed a normal a-wave both in amplitude and implicit time. There was a severely reduced b-wave and a preserved d-wave in keeping with ON-pathway dysfunction with OFF-pathway preservation consistent with the diagnosis of cCSNB.

OFF-Pathway Function Is Altered Amidst Absent ON-Responses in Mice Lacking *Lrit3*

To study the cone-driven ON- and OFF-responses in mice lacking functional LRIT3, we further evaluated these pathways at the level of RGCs by MEA recordings (Fig. 2). In the dark, before the light stimulus, RGCs displayed a spontaneous spiking activity in both wild-type and *Lrit3*$^{nob6/nob6}$ retinas. Spontaneous activity was stable over time in recorded retinas, and no oscillatory activity was observed in both conditions. Immediately after light onset, RGCs of wild-type retinas showed a remarkable increase in their firing rate that rapidly reached a maximum before returning to the baseline (Figs. 2A, 2C), in a characteristic signature of the ON-responses. Upon light offset, a similar profile was observed (Figs. 2A, 2C), reflecting OFF-responses. In *Lrit3*$^{nob6/nob6}$ retinas, the spiking activity remained at the level of the spontaneous activity after light onset, suggesting complete absence of ON-responses of any type, whether transient or sustained (Figs. 2B, 2D). At light offset, the firing rate of RGCs in *Lrit3*$^{nob6/nob6}$ retinas substantially increased, suggesting the presence of OFF-responses. However, reaching the maximum firing rate as well as returning to the baseline appeared to take longer as compared to wild-type retinas (Figs. 2B, 2D). To confirm these observations, two parameters were evaluated for both ON- and OFF-responses: the maximal firing rate and the time at which this maximum was reached for ON-responses after light onset and for OFF-responses after light offset. Compared to

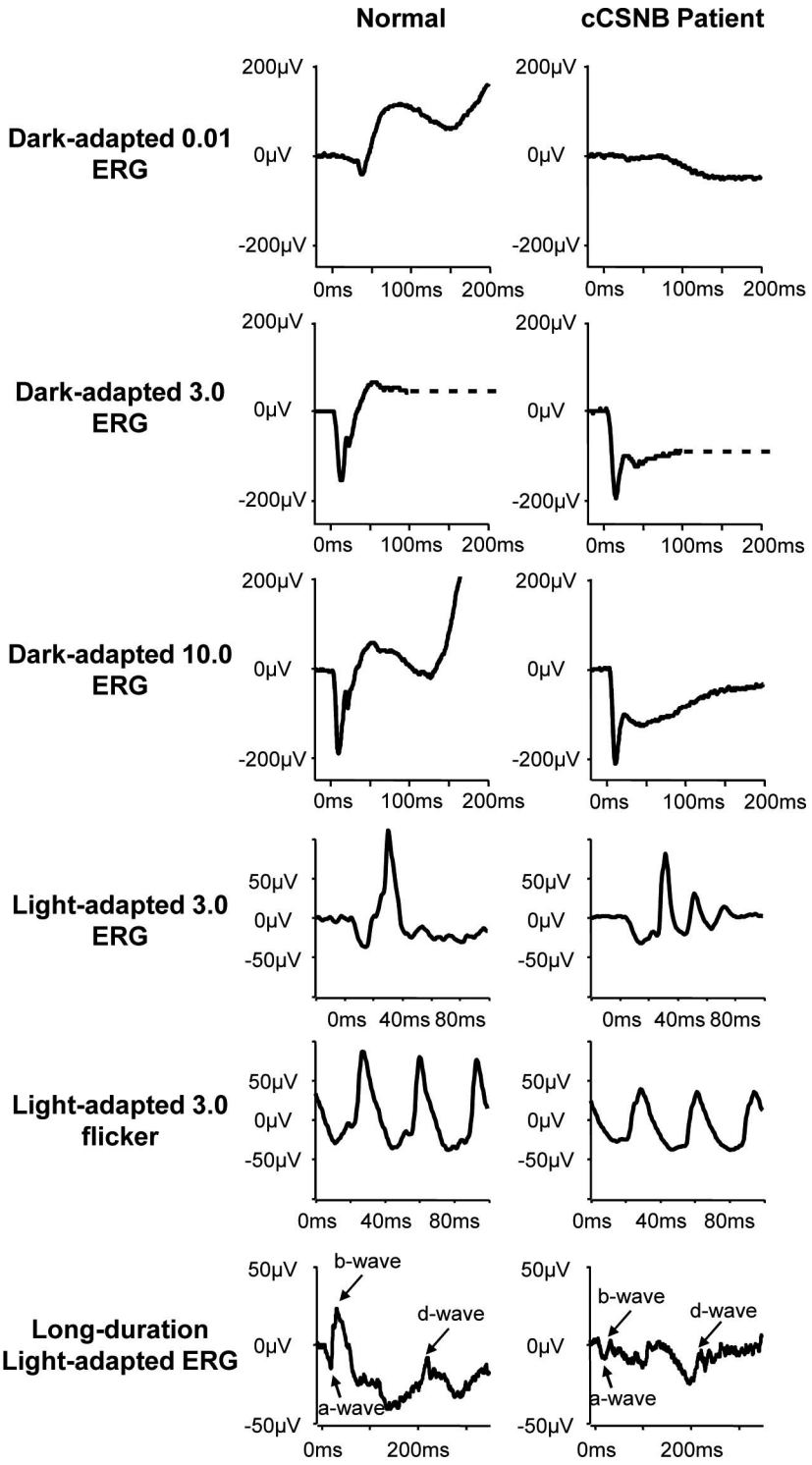

Figure 1. Full-field ERG of the cCSNB patient with *LRIT3* mutations. Electroretinogram traces of the patient affected with cCSNB due to *LRIT3* mutations (*right*) as compared to a normal subject (*left*). No recordable responses for the dark-adapted 0.01 ERG recording were detected. Dark-adapted 3.0 and 10.0 ERGs showed an a-wave with normal implicit time and amplitude but a severely reduced b-wave, leading to an electronegative waveform. Light-adapted 3.0 ERGs showed amplitudes at the lower limit of normal but implicit time shift for both the a-wave and the b-wave. The a-wave had a broadened trough in the patient with *LRIT3* mutations, and there was a sharply rising b-wave with no oscillatory potentials. Light-adapted 3.0 flicker ERGs showed amplitudes at the lower limit of normal but a broadened trough and a mildly delayed implicit time. ON- and OFF-BC recordings revealed a normal a-wave both in amplitude and implicit time. A severely reduced b-wave and a preserved d-wave, in keeping with ON-pathway dysfunction with OFF-pathway preservation, were detected.

Investigative Ophthalmology & Visual Science

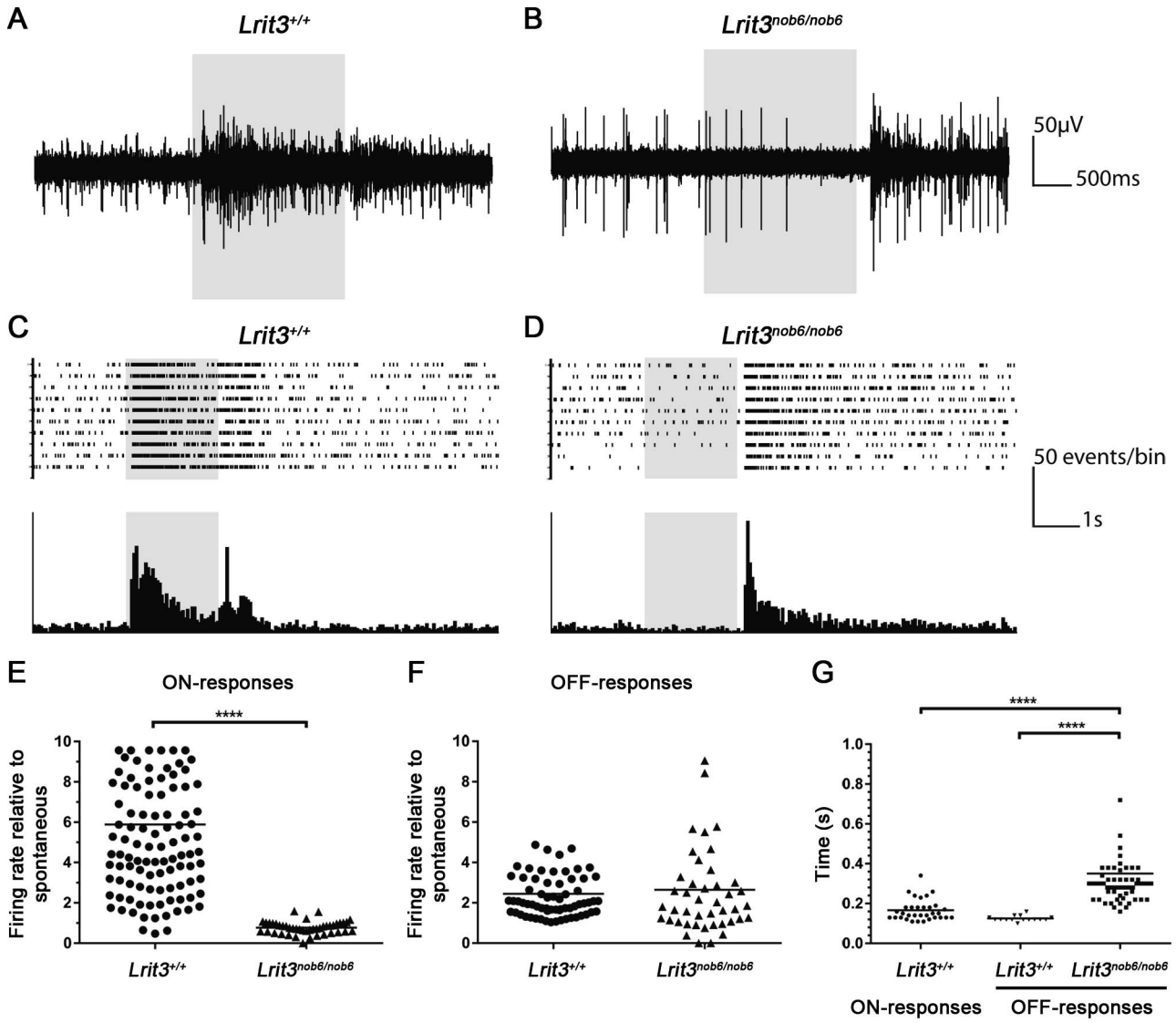

FIGURE 2. ON- and OFF-responses of RGCs in *Lrit3*$^{nob6/nob6}$ retinas. Representative RGC activity recording from an *Lrit3*$^{+/+}$ retina (**A**) and an *Lrit3*$^{nob6/nob6}$ retina (**B**). The gray box corresponds to the light stimulus. *Horizontal scale bar*: 500 ms; *vertical scale bar*: 50 μV. Representative raster plot (*up*) and peristimulus time histogram (*bottom*) from an *Lrit3*$^{+/+}$ retina (**C**) and an *Lrit3*$^{nob6/nob6}$ retina (**D**). The gray box corresponds to the light stimulus. *Horizontal scale bar*: 1 second; *vertical scale bar*: 50 events/bin. Maximum firing rate of ON- (**E**) and OFF-responses (**F**) in *Lrit3*$^{nob6/nob6}$ retinas compared to *Lrit3*$^{+/+}$ retinas relative to the spontaneous activity. *Bars* represent median values. *Asterisks* represent results that are significantly different ($P < 0.05$). (**G**) Time for which the maximum firing rate is reached after the light stimulus onset for ON-responses in *Lrit3*$^{+/+}$ retinas and the light stimulus offset for OFF-responses in *Lrit3*$^{nob6/nob6}$ retinas compared to *Lrit3*$^{+/+}$ retinas. *Bars* represent median values. *Asterisks* represent results that are significantly different ($P < 0.05$).

spontaneous activity of RGCs in wild-type retinas, spiking activity of RGCs increased at light onset and this firing rate for ON-responses reached a maximum that was increased approximately 6-fold. To the contrary, spiking activity of RGCs in *Lrit3*$^{nob6/nob6}$ retinas did not differ from spontaneous activity at light onset (Fig. 2E). The difference between wild-type and *Lrit3*$^{nob6/nob6}$ retinas was statistically significant. The maximum firing rate for OFF-responses did not significantly differ between wild-type and *Lrit3*$^{nob6/nob6}$ retinas and was approximately 2.5 times over the level of spontaneous activity ($P = 0.3811$) (Fig. 2F). However, the time to reach this maximum was significantly increased in *Lrit3*$^{nob6/nob6}$ retinas compared to wild-type retinas, indicating that OFF-responses were delayed in *Lrit3*$^{nob6/nob6}$ retinas (Fig. 2G, Supplementary Fig. S1). Moreover, this parameter was spread in knockout retinas compared to wild-type retinas. We also noticed that the maximal firing rates were similar between ON- and OFF-responses in wild-type retinas (approximately 150 ms) (Fig. 2G). Together, these results showed that, at the level of RGCs, LRIT3 loss abolishes ON-responses and slows the timing of OFF-responses.

Ionotropic Glutamate Receptors and Dystroglycan Receptor Pikachurin Are Normally Localized at Photoreceptor Synapses

To determine whether alterations in the OFF-pathway activity in the absence of LRIT3 are brought about by changes in targeting of ionotropic glutamate receptors to the dendritic tips of OFF-BCs, we studied the localization of GluR1 and GluR5 in the OPL (Fig. 3). GluR1 is an AMPA receptor present at the dendritic tips of type 3b and type 4 OFF-BCs, and GluR5

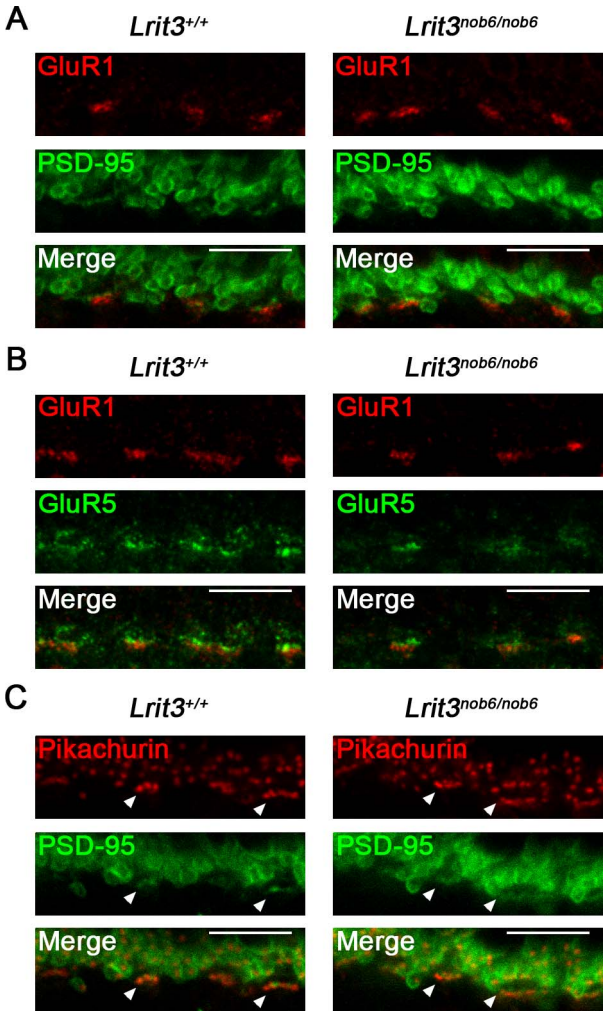

FIGURE 3. Localization of ionotropic glutamate receptors GluR1 and GluR5 and pikachurin in *Lrit3*$^{nob6/nob6}$ retinas. Representative confocal images of cross-sections centered on OPL of *Lrit3*$^{+/+}$ and *Lrit3*$^{nob6/nob6}$ retinas stained with antibodies against (**A**) GluR1 (*red*) and PSD-95 (*green*) and merge, (**B**) GluR1 (*red*) and GluR5 (*green*) and merge, and (**C**) pikachurin (*red*) and PSD-95 (*green*) and merge. *Arrowheads* represent putative cone synapses. *Scale bar*: 10 μm.

is a kainate receptor present at the dendritic tips of type 3a, type 3b, and type 4 OFF-BCs.[8,31] PSD-95 was used as a marker for rod spherules and cone pedicles[32] to identify position of photoreceptor axonal terminals. Both GluR1 and GluR5 antibodies showed a punctate staining clustered as patches in the OPL regions of both wild-type and in *Lrit3*$^{nob6/nob6}$ mice (Figs. 3A, 3B). GluR1 staining was in direct apposition to PSD-95 staining (Fig. 3A), and both GluR5 and GluR1 positive puncta were present at the same cone pedicles (Fig. 3B). Thus, we concluded that targeting of ionotropic glutamate receptors to the dendritic tips of OFF-BCs was unaffected by LRIT3 loss.

We next determined possible changes in synaptic cytoarchitecture by studying localization of pikachurin, a component of the dystrophin–glycoprotein complex, which localizes at the synaptic cleft of both rod and cone synapses and plays an important role in transsynaptic apposition of pre-and postsynaptic compartments[33,34] (Fig. 3). Pikachurin antibody showed punctate staining of two different types in the OPL of both wild-type and *Lrit3*$^{nob6/nob6}$ mice (Fig. 3C): isolated puncta at the synaptic cleft of rod synapses and clustered puncta at the synaptic cleft of cone synapses (Fig. 3C, arrowheads). Pikachurin staining was in direct apposition to PSD-95 staining (Fig. 3C). Thus, we concluded that the loss of LRIT3 has no effect on the localization of pikachurin at the synaptic cleft of both rod and cone synapses.

Rod Synapses Are Morphologically Normal in Retinas Lacking *Lrit3*

Given disruption in the accumulation of synaptic proteins in the OPL of *Lrit3* knockout retinas, we evaluated the morphology of synapses formed by rod and cone photoreceptors by transmission electron microscopy (EM) (Figs. 4, 5). Examination of the rod synapses revealed that retinas of *Lrit3*$^{nob6/nob6}$ mice had regularly shaped and organized rod spherules formed by the axonal terminals of these neurons. We detected no alterations in synaptic ribbons or organelle structure. In immediate apposition to ribbons we detected lateral processes of horizontal cells and deeply invaginating dendrites of the rod BCs. The tips of the ON-BCs were positioned immediately below the ribbons and were properly aligned with respect to the orientation relative to horizontal cell processes (Fig. 4A). On average, 60% of wild-type and 65% of knockout rod spherules from 520 and 436 rod synapses of wild-type and *Lrit3*$^{nob6/nob6}$ mice, respectively, had typical triad configuration containing invaginating ON-BC processes (Fig. 4C). Thus, we concluded that elimination of LRIT3 does not affect the structure of the rod-to-rod BC synapses.

Cone Synapses Have Significantly Less Invaginating Cone ON-BC Dendrites but Show No Decrease in Flat Cone OFF-BC Contacts

Next, we assessed the morphology of synapses formed by cone photoreceptors. Cone axons form substantially larger terminals that stratify in the lower sublamina of the OPL and contain multiple ribbons. Overall, this organization was preserved in *Lrit3*$^{nob6/nob6}$ mice and we could readily identify well-formed cone pedicles at the appropriate location (Fig. 4B). Nevertheless, we noticed frequent appearance of vacuole-like structures in the knockout terminals that we did not observe in the wild-type samples. We found normal-looking ribbons both in terms of number and morphology to be present in *Lrit3*$^{nob6/nob6}$ mice. Furthermore, these ribbons were properly positioned toward the edge of the terminal and contained adjacent horizontal cell processes. In contrast to rod synapses, we observed a marked reduction of the invaginating contacts made by the cone ON-BCs at cone synapses. Quantification of 99 to 108 individual cone pedicles in wild-type and 82 to 123 in *Lrit3*$^{nob6/nob6}$ mice, respectively, confirmed this observation (Fig. 4D). We found a dramatic reduction in the number of triads containing cone ON-BC processes in *Lrit3*$^{nob6/nob6}$ cone pedicles. Quantitatively, 26% of "triads" in cone synapses contained invaginating ON-BC dendrites in wild-type retinas, whereas only ~7% of "triads" in cone synapses contained invaginating ON-BC dendrites in mutant retinas, indicating that there were more diads in mutant retinas than in wild-type retinas. We also observed a substantial increase in the number of flat contacts at the base of cone pedicles, typically observed for OFF-BCs. Because the identity of the BC types cannot be ascertained from morphologic analysis by EM, these flat contacts may correspond to either OFF-BCs or cone ON-BC dendrites incompletely penetrating the cone pedicles and thus positioned farther away from the ribbons. However, despite these deficits we observed a number of normal cone ON-BC–like contacts with *Lrit3*$^{nob6/nob6}$ cone pedicles. To verify the preservation of some invaginating ON-type positioning of

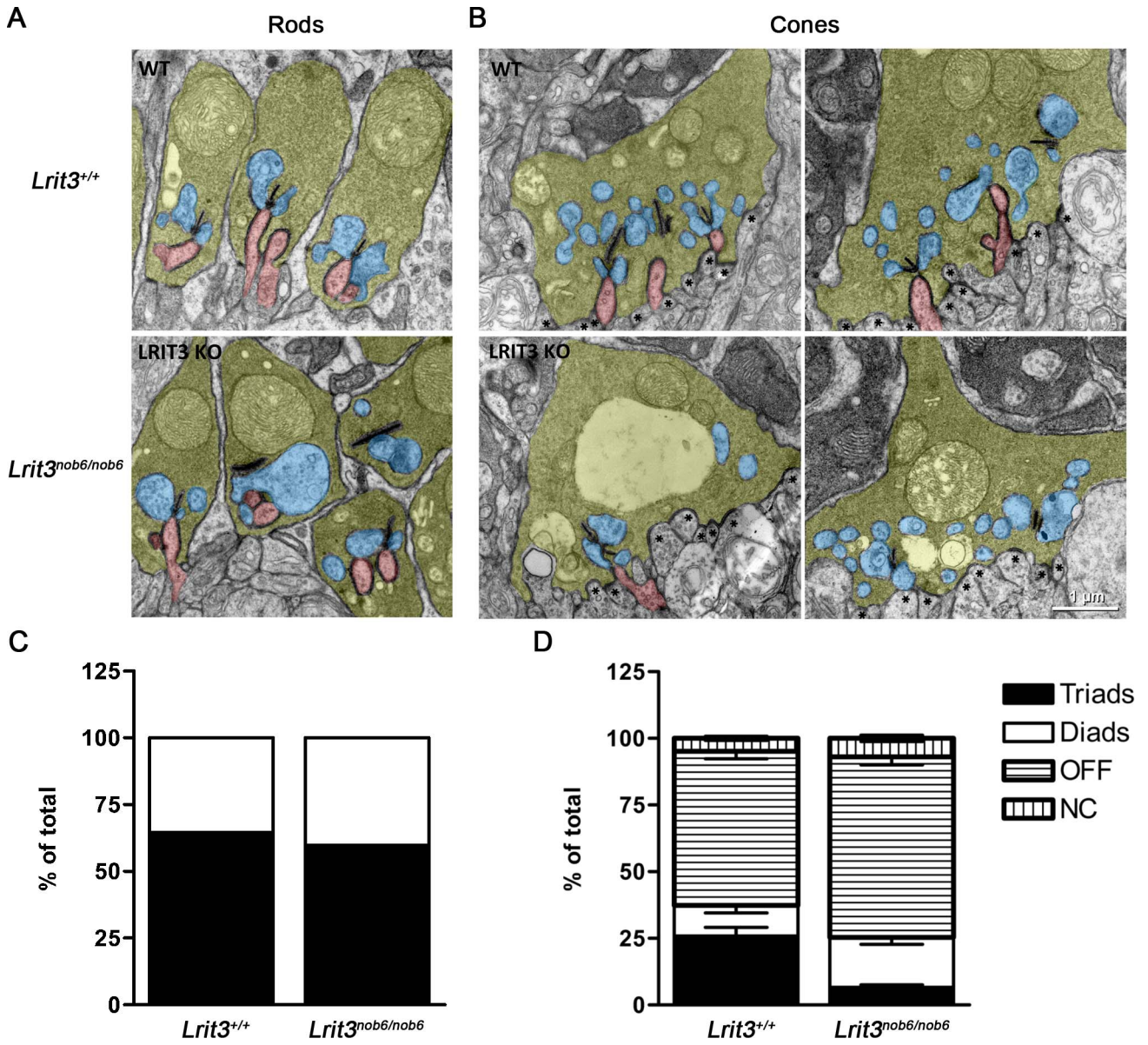

FIGURE 4. Ultrastructure of rod and cone synapses in *Lrit3*$^{nob6/nob6}$ mice. Representative electron microscopy images of rod (**A**) and cone (**B**) ribbon synapses in *Lrit3*$^{nob6/nob6}$ retinas compared to *Lrit3*$^{+/+}$ retinas. Rod spherules and cone pedicles are shown in *yellow*, invaginating dendrites of both rod and cone ON-BCs are shown in *red*, horizontal cell processes are shown in *blue*, and flat-contacting dendrites of cone OFF-BCs are marked with *asterisks*. *Scale bar*: 1 µm. (**C**) Quantification of synaptic elements present in rod spherules. Synapses are classified as diads if they have identifiable ribbon with adjacent horizontal cell process. If spherules additionally have ON-BC process next to the synaptic ribbon, they are designated as triads. (**D**) Quantification of synaptic elements at the cone pedicles of *Lrit3*$^{nob6/nob6}$ retinas compared to *Lrit3*$^{+/+}$ retinas as a percentage of all counted synapses. In addition to diads and triads classified as described above, flat contacts at the base of the pedicle away from the ribbon were also distinguished and labeled as OFF type. Not-otherwise-classified contacts are labeled as NC (not classified). *Error bars* represent standard error of the mean values.

processes within cone terminals, we performed limited serial section observation. A representative panel of serial sections through the same cone pedicle is presented in Figure 5 and provides evidence for cone ON-BC dendrite entering deep into the cone terminal to position itself in apposition to the ribbon (Fig. 5). Thus, despite dramatic reduction in the number of synaptic contacts, some ON-BCs are still capable of establishing normal invaginating synapses with cone terminals. In summary, we detected substantial abnormalities in the organization of the cone synapses with quantitative loss of deeply invaginating contacts made by cone ON-BCs.

DISCUSSION

In this study, we showed that rod synapses in a cCSNB mouse model lacking *Lrit3* (*Lrit3*$^{nob6/nob6}$) are structurally normal. We further detected many normal invaginating contacts formed by cone ON-BC dendrites with cone pedicles. Yet, we also observed a substantial reduction in the number of these synaptic contacts, indicating that while LRIT3 is not absolutely required for cone-to-cone ON-BC synaptogenesis, it plays an important role in this process. Interestingly, this contribution of LRIT3 was remarkably selective, as it did not affect formation of flat contacts between OFF-BC dendrites and cone pedicles.

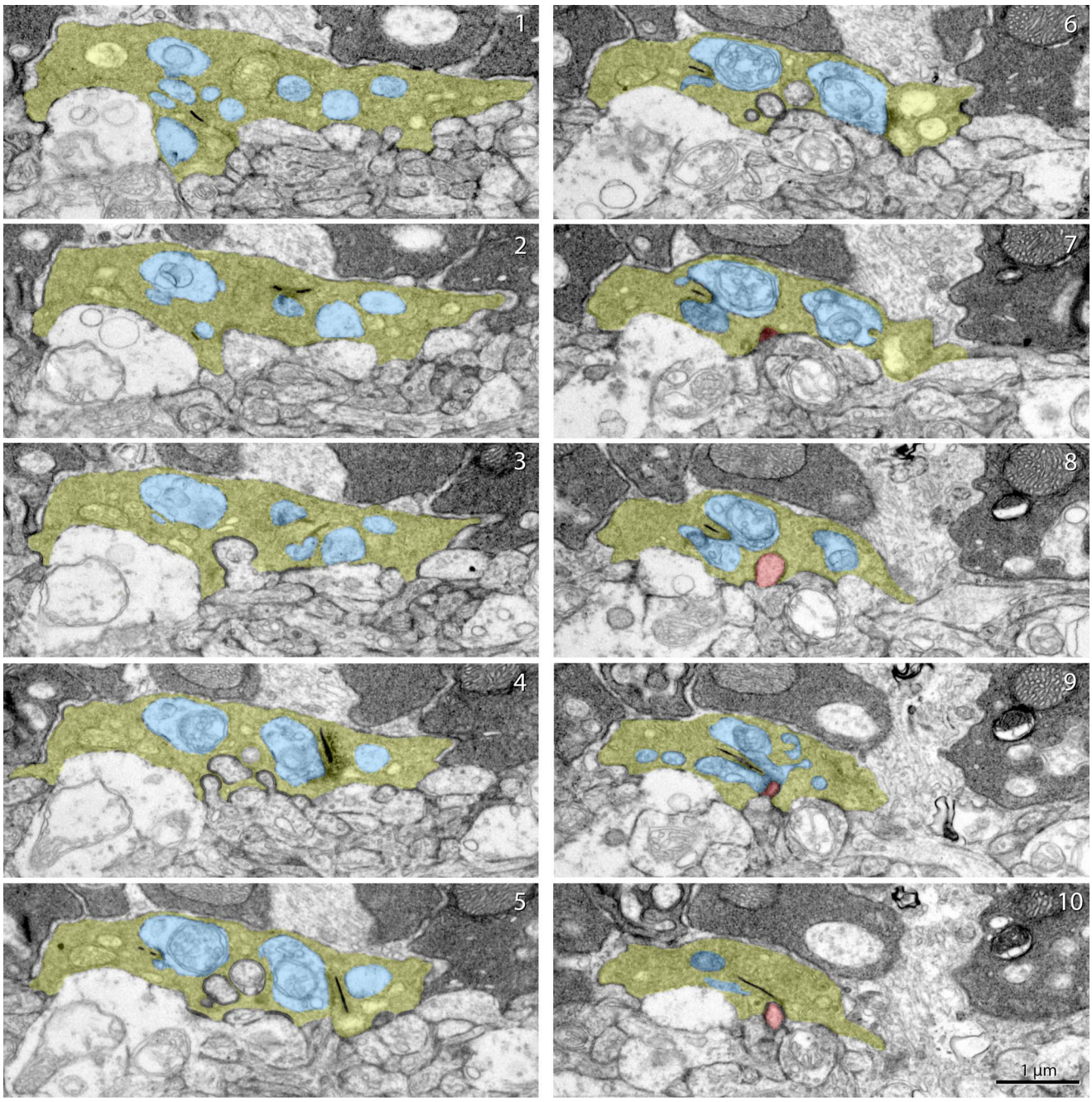

Figure 5. Serial ultrathin section images of a cone pedicle in an *Lrit3*$^{nob6/nob6}$ retina**.** Serial electron microscopy images of a cone pedicle in an *Lrit3*$^{nob6/nob6}$ retina. A gallery shows images of every two sections. Cone pedicle is shown in *yellow*, invaginating dendrite of cone ON-BC is shown in *red*, and horizontal cell processes are shown in *blue. Scale bar*: 1 µm.

Furthermore, absence of LRIT3 did not affect the correct localization of ionotropic glutamate receptors at the dendritic tips of cone OFF-BCs. Functionally, ON-responses were abolished in this cCSNB mouse model and its human cCSNB counterpart; OFF-responses were still present. In the mouse model, we demonstrated that OFF-responses were delayed, which may reflect functional changes in the synaptic transmission.

The structural defects appeared to affect only cone synapses with cone ON-BCs, since OFF-BCs still made flat contacts at cone pedicles in mice lacking *Lrit3*. However, the current study did not discriminate between the effects of LRIT3 on synapse formation versus its maintenance. In the future, it would be interesting to perform an ultrastructural study at an earlier stage in the retinal development to decipher if LRIT3 function is important for the development and/or maintenance of the cone ribbon synapse. Interestingly, structural defects have already been shown in several cCSNB mouse models or in knockout mouse models lacking proteins involved in the mGluR6 signaling cascade.[35–40] However, the present report is the first to observe a structural defect specifically affecting cone, but not rod synapses. These results suggest that LRIT3 may participate in synaptogenesis reactions that are selective for wiring cones.

Interestingly, several proteins have been reported to play a role in rod synapse formation. Proteins of the dystrophin–glycoprotein complex localized in the synaptic cleft of both rod and cone synapses, including dystroglycan and pikachurin, may be involved in the maintenance of a stable adhesion between rod spherules and rod ON-BC dendrites.[40] We evaluated the localization of pikachurin in the OPL of *Lrit3*$^{nob6/nob6}$ mice and showed that pikachurin normally localizes at the synaptic cleft of both rod and cone synapses, indicating that pikachurin is unlikely to be directly involved in the maintenance of the cone ribbon synapse. Similarly, it has been recently shown that a protein, ELFN1, is specifically expressed at the surface of rod spherules where it trans-synaptically interacts with mGluR6, to enable formation of the rod synapse.[39] Interestingly, similarly to LRIT3, ELFN1 contains leucine-rich repeat domains, recently shown to be important for protein–protein interactions and synaptogenesis.[41] Presently, mediators of synaptogenic function of LRIT3 are unknown and their identification by affinity purification/mass spectrometry, for instance, would be an important goal as it may reveal selective transsynaptic mechanisms involved in cone synapse formation.

As expected from the cCSNB phenotype, *Lrit3*$^{nob6/nob6}$ retinas showed no cone-driven ON-responses at the level of ganglion cells. A similar phenotype resulting in the absence of short-latency ON-responses is also observed in other mouse models of cCSNB where components of the mGluR6 cascade are mutated or absent.[18,19,42–44] Thus, our results confirm that the mGluR6 signaling cascade is nonfunctional in mice lacking *Lrit3*. In contrast, the OFF-responses are present and have a normal firing rate in *Lrit3*$^{nob6/nob6}$ mice. Similarly, in other mouse models with cCSNB, the major defect is characterized by the absence of ON-responses and relatively unaffected OFF-responses. However, *Lrit3*$^{nob6/nob6}$ mice also showed OFF-responses, which were significantly delayed in onset latencies. The distribution of latencies clearly indicates a delay in the OFF-responses for most if not all recorded RGCs (Fig. 2G), which may suggest synaptic changes at the photoreceptor to OFF-BC synapse. However, a follow-up study is needed to define if the different types of ganglion cells are differently affected by this latency delay, bearing in mind previous and recent findings showing the existence of at least 32 different types of ganglion cells.[45–53] Of note, in other mouse models with cCSNB, variability in minor altered OFF-responses has been reported.[16,18,19,42–44] These findings show that although the main defect in cCSNB arises from a lack of ON-pathway signaling, the OFF-pathway may also be affected. This situation seems to be strikingly different for mutations in presynaptic proteins present at the photoreceptor terminals and implicated in the incomplete type of CSNB. For example, a mouse model lacking the α-subunit of the calcium channel Cav1.4[54,55] exhibits lack of both ON- and OFF-responses when evaluated at either bipolar or ganglion cell levels.[56,57] Therefore, we think it is likely that the OFF-response deficits observed in the *Lrit3* knockout mouse model represent a secondary effect resulting from the primary alterations in ON-pathways. Indeed, recent studies[42,58] at the level of bipolar or ganglion cells, using different species, contradict the notion that ON- and OFF- signals are truly selective for a single pathway. In addition, crosstalk between ON- and OFF-pathways mediated by amacrine cells has been described in mammalian retinas. Multistratified amacrine cells receive ON-signals via chemical synapses with ON-bipolar cell axon terminals in the inner plexiform layer and then deliver these signals to OFF ganglion cells.[59] This may explain minor altered OFF-responses observed in mouse models with cCSNB. Furthermore, we confirmed that full-field ERG recordings performed according to ISCEV standards in a patient with *LRIT3* mutations display characteristic responses of cCSNB.[24] Namely, there was absence of detectable responses to a dim flash as well as electronegative waveform to a bright flash under scotopic conditions, keeping with rod ON-pathway dysfunction.[60,61] Moreover, photopic ERG responses indicate a selective ON-bipolar pathway dysfunction with OFF-bipolar pathway preservation.[62] We further documented these abnormalities by performing long-duration stimulations, which revealed a normal a-wave but a severely reduced ON–b-wave and a preserved OFF–d-wave. However, long-duration stimulations allow only a qualitative rather than quantitative analysis owing to the high variability for OFF-responses,[63] and we were not able to conclude if these OFF-responses are delayed in the patient as shown for the mouse model. It has been previously demonstrated that photoreceptors release glutamate at synaptic ribbons and that the neurotransmitter subsequently diffuses toward the dendritic tips of OFF-BCs.[64–66] So, the displacement of ON-bipolar dendrites and concomitant increase in the number of flat contacts that we observed in *Lrit3*$^{nob6/nob6}$ mice may affect transmission to OFF-BCs through steric occlusion. Despite the fact that the exact mechanisms underlying deficits in OFF-pathways induced by the loss of LRIT3 function remain to be elucidated, some recent techniques allowing imaging of glutamate release dynamics in the retina[67,68] would be useful to investigate this hypothesis in the future. However, species differences may also account for the observed different onset of the OFF-responses observed in mice lacking LRIT3 and the patient harboring *LRIT3* mutations. Indeed, in general the cone system shows considerable variation across species.[69] This is also highlighted by the different cone ERG waveforms always seen in mouse models for cCSNB compared to patients with the same gene defect. The photopic b-wave seems to be more severley reduced in mouse models than in patients.[26]

In summary, our findings highlight LRIT3 as a molecule important for ON-pathway signaling from both rod and cone photoreceptors to ON-BCs to ON-ganglion cells. Although LRIT3 is important for correctly localizing TRPM1 in the dendritic tips of both rod and cone ON-BCs, it has an additional role in correctly localizing proteins of the same cascade solely in the dendritic tips of cone ON-BCs. This could be related to a role of LRIT3 in cone synapse organization, which regulates the number of synapses made by cone ON-BCs to cone pedicles rather than playing a permissive role in the establishment of the synaptic connectivity per se. These results suggest that LRIT3 is likely involved in coordination of the transsynaptic communication between cones and ON-BCs during synapse formation and function. Further identification of interacting molecules of LRIT3 may shed light on the molecular mechanisms of LRIT3 function.

Acknowledgments

The authors are grateful to the patient and her family for participation in the study, to the platform of animal housing at the Institut de la Vision, to Silke Haverkamp (Max Planck Institute for Brain Research, Frankfurt, Germany) for protocols concerning the OFF-bipolar cell markers, and to Alain Chédotal (Institut de la Vision) for providing the commercial anti–PSD-95 antibody.

Supported by Agence Nationale de la Recherche (ANR-12-BSVS1-0012-01_GPR179) (CZ), Fondation Voir et Entendre (CZ), Prix Dalloz for "la recherche en ophtalmologie" (CZ), Fondation pour la Recherche Médicale (FRM DVS20131228918) in partnership with Fondation Roland Bailly (CZ), Fédération des Aveugles et Amblyopes de France (MN), Ville de Paris and Région Ile de France, LABEX LIFESENSES (reference ANR-10-LABX-65) supported by French state funds managed by the Agence Nationale de la Recherche within the Investissements d'Avenir programme (ANR-

11-IDEX-0004-0), Foundation Fighting Blindness Center Grant (C-CMM-0907-0428-INSERM04), ERC-Synergy HELMHOLTZ (JAS), and Grants EY018139 and DA026405 from the National Institutes of Health, Bethesda, Maryland, United States (KAM). The funders had no role in study design, data collection, analysis and interpretation, decision to publish, or preparation of the manuscript. The authors declare no competing financial interests.

Disclosure: **M. Neuillé**, None; **Y. Cao**, None; **R. Caplette**, None; **D. Guerrero-Given**, None; **C. Thomas**, None; **N. Kamasawa**, None; **J.-A. Sahel**, None; **C.P. Hamel**, None; **I. Audo**, None; **S. Picaud**, None; **K.A. Martemyanov**, None; **C. Zeitz**, None

References

1. Nakajima Y, Iwakabe H, Akazawa C, et al. Molecular characterization of a novel retinal metabotropic glutamate receptor mGluR6 with a high agonist selectivity for L-2-amino-4-phosphonobutyrate. *J Biol Chem*. 1993;268:11868–11873.
2. Nomura A, Shigemoto R, Nakamura Y, Okamoto N, Mizuno N, Nakanishi S. Developmentally regulated postsynaptic localization of a metabotropic glutamate receptor in rat rod bipolar cells. *Cell*. 1994;77:361–369.
3. Masu M, Iwakabe H, Tagawa Y, et al. Specific deficit of the ON response in visual transmission by targeted disruption of the mGluR6 gene. *Cell*. 1995;80:757–765.
4. Morgans CW, Zhang J, Jeffrey BG, et al. TRPM1 is required for the depolarizing light response in retinal ON-bipolar cells. *Proc Natl Acad Sci U S A*. 2009;106:19174–19178.
5. Shen Y, Heimel JA, Kamermans M, Peachey NS, Gregg RG, Nawy S. A transient receptor potential-like channel mediates synaptic transmission in rod bipolar cells. *J Neurosci*. 2009;29:6088–6093.
6. Koike C, Obara T, Uriu Y, et al. TRPM1 is a component of the retinal ON bipolar cell transduction channel in the mGluR6 cascade. *Proc Natl Acad Sci U S A*. 2010;107:332–337.
7. Brandstatter JH, Koulen P, Wassle H. Diversity of glutamate receptors in the mammalian retina. *Vision Res*. 1998;38:1385–1397.
8. Puller C, Ivanova E, Euler T, Haverkamp S, Schubert T. OFF bipolar cells express distinct types of dendritic glutamate receptors in the mouse retina. *Neuroscience*. 2013;243:136–148.
9. Ichinose T, Hellmer CB. Differential signalling and glutamate receptor compositions in the OFF bipolar cell types in the mouse retina. *J Physiol*. 2016;594:883–894.
10. Borghuis BG, Looger LL, Tomita S, Demb JB. Kainate receptors mediate signaling in both transient and sustained OFF bipolar cell pathways in mouse retina. *J Neurosci*. 2014;34:6128–6139.
11. Kolb H. Organization of the outer plexiform layer of the primate retina: electron microscopy of Golgi-impregnated cells. *Philos Trans R Soc Lond B Biol Sci*. 1970;258:261–283.
12. Haverkamp S, Grunert U, Wassle H. The cone pedicle, a complex synapse in the retina. *Neuron*. 2000;27:85–95.
13. Hartline HK. The response of single optic nerve fibers of the vertebrate eye to illumination of the retina. *Am J Physiol*. 1938;121:400–415.
14. Bloomfield SA, Dacheux RF. Rod vision: pathways and processing in the mammalian retina. *Prog Retin Eye Res*. 2001;20:351–384.
15. Kuffler SW. Discharge patterns and functional organization of mammalian retina. *J Neurophysiol*. 1953;16:37–68.
16. Pardue MT, McCall MA, LaVail MM, Gregg RG, Peachey NS. A naturally occurring mouse model of X-linked congenital stationary night blindness. *Invest Ophthalmol Vis Sci*. 1998;39:2443–2449.
17. Gregg RG, Mukhopadhyay S, Candille SI, et al. Identification of the gene and the mutation responsible for the mouse nob phenotype. *Invest Ophthalmol Vis Sci*. 2003;44:378–384.
18. Pinto LH, Vitaterna MH, Shimomura K, et al. Generation, identification and functional characterization of the nob4 mutation of Grm6 in the mouse. *Vis Neurosci*. 2007;24:111–123.
19. Maddox DM, Vessey KA, Yarbrough GL, et al. Allelic variance between GRM6 mutants, Grm6nob3 and Grm6nob4 results in differences in retinal ganglion cell visual responses. *J Physiol*. 2008;586:4409–4424.
20. Peachey NS, Pearring JN, Bojang P Jr, et al. Depolarizing bipolar cell dysfunction due to a Trpm1 point mutation. *J Neurophysiol*. 2012;108:2442–2451.
21. Peachey NS, Ray TA, Florijn R, et al. GPR179 is required for depolarizing bipolar cell function and is mutated in autosomal-recessive complete congenital stationary night blindness. *Am J Hum Genet*. 2012;90:331–339.
22. Qian H, Ji R, Gregg RG, Peachey NS. Identification of a new mutant allele, Grm6(nob7), for complete congenital stationary night blindness. *Vis Neurosci*. 2015;32:E004.
23. Charette JR, Samuels IS, Yu M, et al. A chemical mutagenesis screen identifies mouse models with ERG defects. *Adv Exp Med Biol*. 2016;854:177–183.
24. Zeitz C, Jacobson SG, Hamel CP, et al. Whole-exome sequencing identifies LRIT3 mutations as a cause of autosomal-recessive complete congenital stationary night blindness. *Am J Hum Genet*. 2013;92:67–75.
25. Neuille M, El Shamieh S, Orhan E, et al. Lrit3 deficient mouse (nob6): a novel model of complete congenital stationary night blindness (cCSNB). *PLoS One*. 2014;9:e90342.
26. Zeitz C, Robson AG, Audo I. Congenital stationary night blindness: an analysis and update of genotype-phenotype correlations and pathogenic mechanisms. *Prog Retin Eye Res*. 2015;45C:58–110.
27. Neuille M, Morgans CW, Cao Y, et al. LRIT3 is essential to localize TRPM1 to the dendritic tips of depolarizing bipolar cells and may play a role in cone synapse formation. *Eur J Neurosci*. 2015;42:1966–1975.
28. McCulloch DL, Marmor MF, Brigell MG, et al. ISCEV standard for full-field clinical electroretinography (2015 update). *Doc Ophthalmol*. 2015;130:1–12.
29. Audo I, Robson AG, Holder GE, Moore AT. The negative ERG: clinical phenotypes and disease mechanisms of inner retinal dysfunction. *Surv Ophthalmol*. 2008;53:16–40.
30. Mace E, Caplette R, Marre O, et al. Targeting channelrhodopsin-2 to ON-bipolar cells with vitreally administered AAV restores ON and OFF visual responses in blind mice. *Mol Ther*. 2015;23:7–16.
31. Hack I, Frech M, Dick O, Peichl L, Brandstatter JH. Heterogeneous distribution of AMPA glutamate receptor subunits at the photoreceptor synapses of rodent retina. *Eur J Neurosci*. 2001;13:15–24.
32. Koulen P, Fletcher EL, Craven SE, Bredt DS, Wassle H. Immunocytochemical localization of the postsynaptic density protein PSD-95 in the mammalian retina. *J Neurosci*. 1998;18:10136–10149.
33. Sato S, Omori Y, Katoh K, et al. Pikachurin, a dystroglycan ligand, is essential for photoreceptor ribbon synapse formation. *Nat Neurosci*. 2008;11:923–931.
34. Omori Y, Araki F, Chaya T, et al. Presynaptic dystroglycan-pikachurin complex regulates the proper synaptic connection between retinal photoreceptor and bipolar cells. *J Neurosci*. 2012;32:6126–6137.
35. Rao A, Dallman R, Henderson S, Chen CK. Gbeta5 is required for normal light responses and morphology of retinal ON-bipolar cells. *J Neurosci*. 2007;27:14199–14204.

36. Cao Y, Masuho I, Okawa H, et al. Retina-specific GTPase accelerator RGS11/G beta 5S/R9AP is a constitutive heterotrimer selectively targeted to mGluR6 in ON-bipolar neurons. *J Neurosci*. 2009;29:9301–9313.
37. Tsukamoto Y, Omi N. Effects of mGluR6-deficiency on photoreceptor ribbon synapse formation: comparison of electron microscopic analysis of serial sections with random sections. *Vis Neurosci*. 2014;31:39–46.
38. Dhingra A, Ramakrishnan H, Neinstein A, et al. Gbeta3 is required for normal light ON responses and synaptic maintenance. *J Neurosci*. 2012;32:11343–11355.
39. Cao Y, Sarria I, Fehlhaber KE, et al. Mechanism for selective synaptic wiring of rod photoreceptors into the retinal circuitry and its role in vision. *Neuron*. 2015;87:1248–1260.
40. Tummala SR, Dhingra A, Fina ME, Li JJ, Ramakrishnan H, Vardi N. Lack of mGluR6-related cascade elements leads to retrograde trans-synaptic effects on rod photoreceptor synapses via matrix-associated proteins. *Eur J Neurosci*. 2016;43:1509–1522.
41. de Wit J, Ghosh A. Control of neural circuit formation by leucine-rich repeat proteins. *Trends Neurosci*. 2014;37:539–550.
42. Renteria RC, Tian N, Cang J, Nakanishi S, Stryker MP, Copenhagen DR. Intrinsic ON responses of the retinal OFF pathway are suppressed by the ON pathway. *J Neurosci*. 2006;26:11857–11869.
43. Demas J, Sagdullaev BT, Green E, et al. Failure to maintain eye-specific segregation in nob, a mutant with abnormally patterned retinal activity. *Neuron*. 2006;50:247–259.
44. Gregg RG, Kamermans M, Klooster J, et al. Nyctalopin expression in retinal bipolar cells restores visual function in a mouse model of complete X-linked congenital stationary night blindness. *J Neurophysiol*. 2007;98:3023–3033.
45. Werblin FS, Dowling JE. Organization of the retina of the mudpuppy, Necturus maculosus, II: intracellular recording. *J Neurophysiol*. 1969;32:339–355.
46. Cleland BG, Levick WR. Brisk and sluggish concentrically organized ganglion cells in the cat's retina. *J Physiol*. 1974;240:421–456.
47. Barlow HB, Hill RM, Levick WR. Retinal ganglion cells responding selectively to direction and speed of image motion in the rabbit. *J Physiol*. 1964;173:377–407.
48. Farrow K, Masland RH. Physiological clustering of visual channels in the mouse retina. *J Neurophysiol*. 2011;105:1516–1530.
49. Coombs J, van der List D, Wang GY, Chalupa LM. Morphological properties of mouse retinal ganglion cells. *Neuroscience*. 2006;140:123–136.
50. Sumbul U, Song S, McCulloch K, et al. A genetic and computational approach to structurally classify neuronal types. *Nat Commun*. 2014;5:3512.
51. Volgyi B, Chheda S, Bloomfield SA. Tracer coupling patterns of the ganglion cell subtypes in the mouse retina. *J Comp Neurol*. 2009;512:664–687.
52. Kong JH, Fish DR, Rockhill RL, Masland RH. Diversity of ganglion cells in the mouse retina: unsupervised morphological classification and its limits. *J Comp Neurol*. 2005;489:293–310.
53. Baden T, Berens P, Franke K, Roman Roson M, Bethge M, Euler T. The functional diversity of retinal ganglion cells in the mouse. *Nature*. 2016;529:345–350.
54. Specht D, Wu SB, Turner P, et al. Effects of presynaptic mutations on a postsynaptic Cacna1s calcium channel colocalized with mGluR6 at mouse photoreceptor ribbon synapses. *Invest Ophthalmol Vis Sci*. 2009;50:505–515.
55. Michalakis S, Shaltiel L, Sothilingam V, et al. Mosaic synaptopathy and functional defects in Cav1.4 heterozygous mice and human carriers of CSNB2. *Hum Mol Genet*. 2014;23:1538–1550.
56. Knoflach D, Schicker K, Glosmann M, Koschak A. Gain-of-function nature of Cav1.4 L-type calcium channels alters firing properties of mouse retinal ganglion cells. *Channels (Austin)*. 2015;9:298–306.
57. Tanimoto N, Michalakis S, Weber BH, Wahl-Schott CA, Hammes HP, Seeliger MW. In-depth functional diagnostics of mouse models by single-flash and flicker electroretinograms without adapting background illumination. *Adv Exp Med Biol*. 2016;854:619–625.
58. Khan NW, Kondo M, Hiriyanna KT, Jamison JA, Bush RA, Sieving PA. Primate retinal signaling pathways: suppressing ON-pathway activity in monkey with glutamate analogues mimics human CSNB1-NYX genetic night blindness. *J Neurophysiol*. 2005;93:481–492.
59. Farajian R, Pan F, Akopian A, Volgyi B, Bloomfield SA. Masked excitatory crosstalk between the ON and OFF visual pathways in the mammalian retina. *J Physiol*. 2011;589:4473–4489.
60. Schubert G, Bornschein H. Analysis of the human electroretinogram [in German]. *Ophthalmologica*. 1952;123:396–413.
61. Miyake Y, Yagasaki K, Horiguchi M, Kawase Y, Kanda T. Congenital stationary night blindness with negative electroretinogram: a new classification. *Arch Ophthalmol*. 1986;104:1013–1020.
62. Miyake Y, Horiguchi M, Terasaki H, Kondo M. Scotopic threshold response in complete and incomplete types of congenital stationary night blindness. *Invest Ophthalmol Vis Sci*. 1994;35:3770–3775.
63. Alexander KR, Fishman GA, Barnes CS, Grover S. On-response deficit in the electroretinogram of the cone system in X-linked retinoschisis. *Invest Ophthalmol Vis Sci*. 2001;42:453–459.
64. Raviola E, Gilula NB. Intramembrane organization of specialized contacts in the outer plexiform layer of the retina: a freeze-fracture study in monkeys and rabbits. *J Cell Biol*. 1975;65:192–222.
65. DeVries SH, Li W, Saszik S. Parallel processing in two transmitter microenvironments at the cone photoreceptor synapse. *Neuron*. 2006;50:735–748.
66. Regus-Leidig H, Brandstatter JH. Structure and function of a complex sensory synapse. *Acta Physiol (Oxf)*. 2012;204:479–486.
67. Borghuis BG, Marvin JS, Looger LL, Demb JB. Two-photon imaging of nonlinear glutamate release dynamics at bipolar cell synapses in the mouse retina. *J Neurosci*. 2013;33:10972–10985.
68. Marvin JS, Borghuis BG, Tian L, et al. An optimized fluorescent probe for visualizing glutamate neurotransmission. *Nat Methods*. 2013;10:162–170.
69. Evers HU, Gouras P. Three cone mechanisms in the primate electroretinogram: two with, one without off-center bipolar responses. *Vision Res*. 1986;26:245–254.

Investigative Ophthalmology & Visual Science